Colloidal glasses under shear strain

M. D. Haw,* W. C. K. Poon, and P. N. Pusey
Department of Physics and Astronomy, The University of Edinburgh, King's Buildings, Mayfield Road, Edinburgh EH9 3JZ, United Kingdom

P. Hebraud and F. Lequeux
Laboratoire de Dynamique des Fluides Complexes, 3 Rue Universite, F-67070 Strasbourg, France
(Received 3 April 1998)

We have studied the effects of oscillatory shear strain on the structure of a colloidal hard-sphere glass. By light scattering, we measure the kinetic development of ordered structures induced by shearing between parallel plates. Diffusing wave spectroscopy ''echo'' experiments show that for peak to peak oscillatory strain below around 30% the colloidal glass strains approximately *reversibly*. At higher strains a partly ordered structure develops, the kinetics of the ordering being strongly dependent on strain. Kinetic measurements demonstrate an ''induction'' time for crystallization with a divergentlike behavior as strain decreases toward $\sim 25-30$ %. We compare the behavior of glassy samples with that of samples at lower volume fraction, where in equilibrium without shear the sample is fully (poly)crystalline. At the lower volume fraction, irreversible yielding is observed at lower strains. There appears some tendency for very high volume fraction glass samples to ''fracture.'' Similar evidence of fracture is not observed at the lower volume fractions. [S1063-651X(98)01010-1]

PACS number(s): 82.70.Dd, 81.40.−z, 83.20.Hn

I. INTRODUCTION

There is substantial current interest in the structure, dynamics, and rheology of so-called ''glassy states'' of mesoscopic matter, for example dense emulsions, foams, and dense colloidal (i.e., solid particle) suspensions. In particular, recent studies of the behavior of glasses subjected to strain include the diffusing wave spectroscopy (DWS) ''echo'' experiments of Hebraud *et al.* [1], where a dense system of deformable emulsion droplets was subjected to small oscillatory (peak to peak) strain amplitudes up to $\gamma \sim 18\%$. Interestingly, at low strains $\gamma \lesssim 10\%$ these ''soft'' glasses showed a localized yielding behavior, where parts of the sample always yielded while other parts continued to strain reversibly over subsequent cycles of oscillatory shear. The question immediately arises whether this localized yielding is particular to glasses of deformable particles, or whether it is common to mesoscopic glasses in general.

Meanwhile, the structural effects of the application of shear to colloidal suspensions have been studied in great detail. Controlled shear strain induces crystallization of suspensions due to the greater ''ease'' of straining in an ordered, oriented suspension (particle collisions are less frequent in the ordered sample) [2]. In particular, the shear-induced crystallization of colloidal particles with hard-sphere-like interactions has been studied by light scattering [3,4] and by optical microscopy [5]. Application of *oscillatory* shear allows samples to be subjected for long times to ''low'' strains (i.e., peak to peak strain amplitudes) $\gamma < 100\%$. The structure induced by the shear at low strain amplitude is quite different to that observed at high strain amplitude (and in steady continuous shear, where γ soon exceeds 100%). At $\gamma \lesssim 100\%$ the suspension is expected to strain most easily by ordering into hexagonal planes in the velocity-vorticity plane, the planes being oriented such that a close packed direction in the hexagonal plane is *perpendicular* to the velocity axis (Fig. 1). In fact experiments have demonstrated that there remains a marked ''polycrystallinity'' or ''mosaicity'' in the structure of the planes, the planes being made up of ''grains'' whose orientations can vary substantially [4–6]. This is in contrast to the case of $\gamma > 100\%$ (and in steady shear), where no such ''mosaicity'' is observed [3,5] (and where the orientation is such that the close-packed direction in the hexagonal plane is *parallel* to the velocity axis).

Suspensions of sterically stabilized poly(methylmethacrylate) (PMMA) particles have been shown to be a good experimental example of the ''model'' hard sphere system [7]. The hard sphere equilibrium phase diagram features

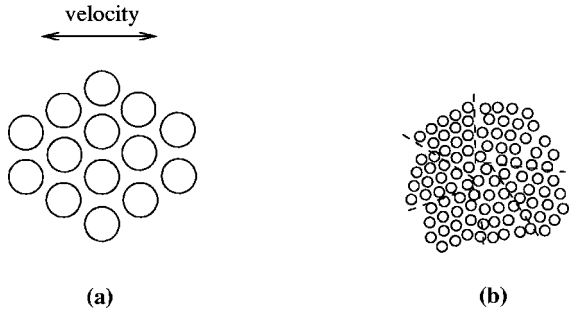

FIG. 1. Schematic picture of ''low strain'' order in the velocity-vorticity plane of a sheared suspension. (a) A single small hexagonal ''crystallite'' is shown with a close packed direction perpendicular to the velocity axis. (b) The typical ''polycrystalline'' or mosaic structure of grains with a distribution of orientations, peaked with a close packed direction perpendicular to the velocity.

*Present address: CEMEF, Ecole des Mines de Paris, 06904 Sophia Antipolis Cedex, France.

a colloidal fluid phase at volume fractions $\Phi<\Phi_f\simeq 0.494$, coexisting fluid and crystalline phases for $\Phi_f<\Phi<\Phi_m \simeq 0.545$, and a fully crystalline phase for $\Phi>\Phi_m$. In the experimental system, at $\Phi>\Phi_g\simeq 0.58$, homogeneous nucleation of crystals is inhibited, and the sample remains in a disordered ''glassy'' state. Dynamic light scattering experiments have shown that the suppression of homogeneous nucleation coincides with the cessation of long-time diffusive motion of the particles, as they are trapped in long-lived neighbor ''cages'' [8].

Ackerson made a comprehensive study of the oscillatory shear-induced crystallization behavior of PMMA samples in the equilibrium coexistence and crystalline regions of the phase diagram [3]. However, little is known of the behavior of hard-sphere *glasses*, i.e., samples with $\Phi>\Phi_g$, especially for ''low'' strains $\gamma\ll 100\%$. Furthermore there have been few reported attempts to study more quantitatively the kinetic growth of shear-induced order. In this paper we use the technique of DWS echo to compare the low-strain behavior of the hard-sphere glass and the soft emulsion glasses studied by Hebraud *et al.* Further, we use conventional time-resolved static light scattering to compare the kinetics of shear-induced ordering in the PMMA glasses with the kinetics of ordering in samples below the glass transition at Φ_g. Additionally, we use optical microscopy to demonstrate qualitatively the evolution of the structure of the glassy samples during shear.

II. METHODS

A. Shear cell and samples

In the experiments described here, spherical PMMA particles sterically stabilized by grafted chains of poly(hydroxystearic) acid (PHSA) are suspended in *cis*-decalin. The particles used in the DWS experiments have radii $a=515\pm 10$ nm, while those used in the time-resolved light scattering and microscopy experiments have $a=485\pm 10$ nm, as determined by static light scattering, with in both cases a size polydispersity of approximately 5%. (Note that the PHSA stabilizing layer has a typical thickness of about 10 nm.) The equilibrium (zero-shear) phase behavior of the PMMA suspensions coincides well with the model hard-sphere system, showing fluid, coexisting crystal and fluid, and fully crystalline phases as described above. Samples at known particle volume fractions Φ are made up as described in detail elsewhere [9]. Briefly, the volume fraction of a stock solution in the fluid-crystal coexistence region of the phase diagram is determined from the relative amounts of the two phases, assuming that the freezing volume fraction (where the crystal phase first appears) Φ_f coincides with the hard-sphere value $\Phi_f=0.494$. Samples at higher volume fractions are made up from the stock solution by centrifuging and removing small amounts of supernatant solvent. Note that using this procedure we observe a melting volume fraction (where the sample is first fully crystalline) $\Phi_m=0.545\pm 0.003$, in good agreement with the hard-sphere value for Φ_m. As in previous work [8], we observe the cessation of homogeneously nucleated crystallization at $\Phi>\Phi_g\simeq 0.58$.

For the experiments, samples are made up in 3-ml sealed cuvettes, from which drops are taken for loading into the shear cell. The shear cell is shown schematically in Fig. 2.

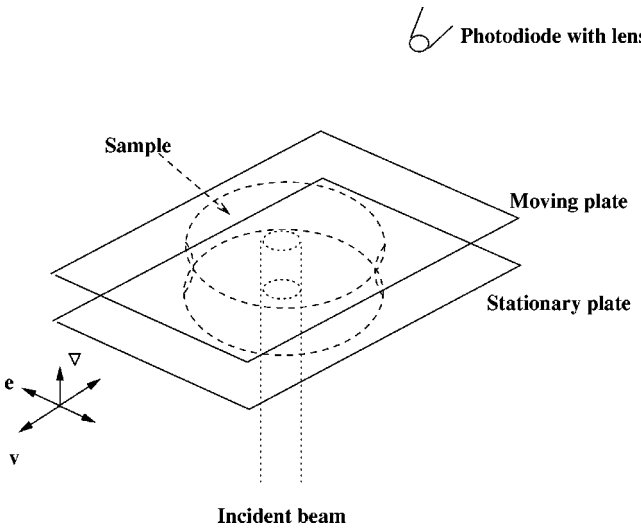

FIG. 2. Schematic of the shear cell, including the positioning of the photodiode in the time-resolved static light-scattering measurements. The sample is typically 1.5–2 cm in diameter. In the DWS-echo experiments the plate separation is 2 mm; in the time-resolved light scattering and optical microscopy experiments the plate separation is typically 520–680 μm. The figure also shows the velocity (**v**), shear gradient (∇), and vorticity (**e**) directions.

Two slightly different cells have been used, one for the DWS-echo experiments (see below) and a second for the time-resolved static light scattering. Both cells consist of parallel flat glass plates, independently fixed to maintain constant plate spacing, the top plate being mounted on bearings such that it may slide back and forth above the stationary bottom plate with minimal friction. The sample is loaded by pipette and forms a drop of diameter typically 15–20 mm between the plates, as shown in Fig 2. In the scattering experiments, the (expanded) beam passes through the center of the drop, the edge of the beam being always at least 5 mm (or about 5000 particle diameters) from the edge of the drop. Optical microscopy indicates no visible effect of the edges of the drop beyond ~ 1 mm from the edge. In both experiments, the cells are mounted in a small closed environment containing surplus solvent which is allowed to evaporate, generating a solvent-saturated atmosphere and minimizing solvent evaporation from the sample itself, over the time scale of the experiments. The DWS-echo cell is driven by a piezoelectric device, together with (for peak to peak amplitudes larger than 100 μm) an amplifying lever, as described in Ref. [1]. The peak to peak amplitude A is measured by a linear variable differential transformer. The gap width between the plates in the DWS-echo cell is $h=2$ mm. In the static light scattering experiments the shear plate is oscillated by means of an electromagnetic vibrator driven by a signal generator. The peak to peak amplitude A is determined by measuring the movement of a marker with a video camera and high magnification zoom lens. The gap width h between the plates, measured by optical microscope, varies slightly from experiment to experiment, between 520 and 680 μm. In both experiments the peak to peak strain γ is given by $\gamma=A/h$.

The density of the PMMA particles is slightly greater than that of the solvent; thus we expect some slow sedimentation of the particles. While a free particle in a dilute solution

would sediment quite quickly, in the dense suspensions considered here sedimentation is much slower. Microscopic observations indicate that sedimentation does not become visibly apparent (i.e., from an apparent reduction in sample density near the top of the shear cell) for times less than about 90 min with the particle sizes, solvent and volume fractions considered here [5]. Thus we do not consider experiments of duration greater than an hour or so in this work. Samples in solvent mixtures whose average density is matched to that of the particles could be used in longer-term experiments and to study the effects of gravity on crystallization both with and without shear [10]. The behavior of PMMA particles in such a mixture of solvents is currently under investigation [11].

B. DWS-echo experiment

We have studied the structural response of the PMMA glasses at low peak to peak strains γ up to $\gamma \sim 50\%$ using the DWS-echo apparatus at the Laboratoire de Dynamique des Fluides Complexes in Strasbourg. Details of the principles of the method and of the experimental setup have been given previously [1,12]. We give a brief description of the concept of the experiment here. The structure of the suspension at any point in the oscillation cycle may be compared with the structure at the same point in subsequent cycles by correlating the light scattered by the structure over the subsequent cycles. A correlator with a fully programmable set of delay times τ, connected to a photomultiplier measuring forward scattering [1], constructs the intensity autocorrelation function $g_2(\tau)$ for τ corresponding to times around the period of oscillation, i.e., $\tau = 1$ cycle, $\tau = 2$ cycles, . . . , $\tau = m$ cycles. Peaks or ''echoes'' thus appear in the correlated signal. The height of the echoes relative to the initial height $g_2(\tau \rightarrow 0)$ is an indication of the degree of irreversible structural change over the given number of cycles. For completely reversible straining of the sample, and in the absence of other disordering processes such as thermal diffusion, the echo height would remain unchanged at $g_2(\tau = m \text{ cycles}) = 1$, where m is an integer. Conversely, decay of the echoes indicates irreversible structural changes taking place over the delay time τ.

The method is sensitive to structural changes on length scales $l > \lambda/n$, where n is the typical number of times a photon is scattered [12]. In the experiments the PMMA particles are suspended in *cis*-decalin, whose refractive index is approximately 1.481, while the effective particle refractive index is $\simeq 1.49$. For a 2-mm-thick sample at the high volume fractions considered here, the transmission coefficient is estimated to be no more than $T = I_T/I_0 \sim \exp(-n) \sim 0.01$. (In practice, no transmitted or unscattered part of the incident beam is visible.) This implies that each photon scatters at least on the order of five times, or that the method resolves structural changes on length scales down to a fifth of the wavelength, $\lambda = 488$ nm. The particle radius in the DWS-echo experiments is $r = 515$ nm, so that the measurements are sensitive to structural changes on length scales down to about a fifth of a particle radius.

C. Time-resolved light scattering

Extensive light scattering studies of the ordering effects of oscillatory shear of PMMA colloids, for the most part on samples below the glass transition volume fraction Φ_g, have been described by Ackerson and co-workers [3,4]. For low peak to peak strains $\gamma < 100\%$, with a beam incident perpendicular to the velocity-vorticity plane (i.e., parallel to the velocity gradient direction) hexagonally arranged bright ''lobes'' are typically observed on a screen placed perpendicular to the incident direction. Figure 3 shows the typical development of the scattering pattern (at one extreme of the oscillation cycle) during an experiment. At the opposite extreme of the cycle the alternate set of three lobes (making up the other three points of the hexagonal pattern) is seen, so that the two sets of three lobes flash on and off alternately as the sample is sheared back and forth. The developing bright ''lobes'' indicate the development of hexagonally ordered planes of particles in the velocity-vorticity plane. The orientation of the pattern indicates that the hexagonally ordered regions have a distribution of orientations of close packed directions, the distribution being peaked perpendicular to the velocity axis. Optical microscopy has been used to confirm the hypothesis [3,4] that the presence of spread-out lobes, as opposed to sharp Bragg peaks, results from such a partly polycrystalline or mosaic structure, consisting of grains with a narrow distribution of close packed directions peaked perpendicular to the velocity axis [5]. It is worth pointing out that our scattering observations in the parallel flat plate geometry match those of previous experiments in both the double-Couette-cylinder geometry [3,4] and (for a different system of colloids) in the rotating parallel disc geometry [13].

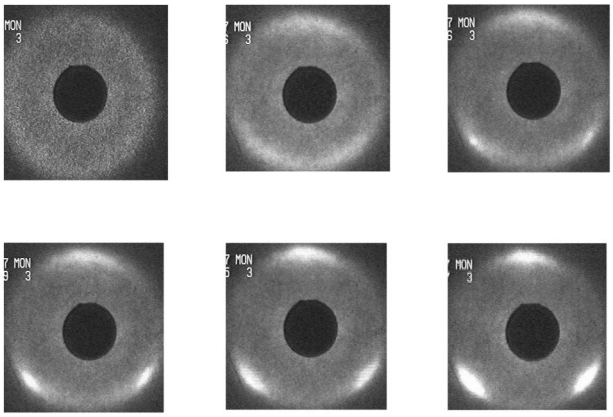

FIG. 3. Evolution of the scattering pattern as imaged on a paper screen, for an experiment at strain $\gamma = 57\%$, frequency $f = 5$ Hz, on a sample at volume fraction $\Phi = 0.587$. The pictures are digitized from video, the camera being on the axis of the incident beam, i.e., the shear gradient direction. The velocity direction is vertical in the pictures. Each frame is taken close to the same extreme of the shear cycle (when the top plate is furthest toward the top of the picture). The first picture (top left) shows the pattern before starting the shear. Subsequent times are (top row) 1 min 35 s, 4 min; (bottom row) 5 min 30 s, 8 min 30 s, and 17 min 15 s.

In order to obtain more quantitative information about the growth of crystalline order in the sheared suspensions, we have measured the increase in time of the scattering intensity near the center of the lobe on the velocity axis, by positioning a photodiode at the lobe as shown in Fig. 2. An expanded laser beam of circular cross section (diameter approximately 5 mm) and *in vacuo* wavelength $\lambda = 633.8$ nm is directed

into the sample perpendicular to the velocity-vorticity plane (the plane of the glass plates of the cell). Note that we use a small lens across the front of the photodiode, so that scattered light is collected from an area approximately 0.2 mm^2. Thus the measurements effectively average over a small region of reciprocal space near the scattering peak. The output voltage of the diode is measured over time as the sample is subjected to oscillatory shear. In practice we observe peaks in the output voltage during a cycle, corresponding to the ''flashing'' of the scattering peak as the growing planes are brought into and taken out of strong scattering configurations by the action of the shear. Thus we record the increase of the peak voltage with time, and take this as a measure of the increasing order within the sample. While this measurement remains only semiquantitative (for instance, we have ignored the possible effects of multiple scattering) the behavior of the measured voltage over time will still demonstrate approximately the kinetics of the growth of structure within the sheared suspension. As far as multiple scattering is concerned, it should be noted that in the time-resolved scattering experiments the thickness of the sample (the separation between the plates of the shear cell) is typically only a quarter that of the samples in the DWS-echo experiments, so that in the time-resolved scattering experiments single scattering remains dominant.

The assumption is often made in *neutron* scattering experiments on colloids under shear that, when the incident beam is perpendicular to the velocity-vorticity plane, the collected scattering pattern is in the velocity-vorticity plane of reciprocal space, or in other words that the component of the scattering vector in the velocity gradient direction, k_∇, is zero [14]. However, this is only a reasonable approximation for small angles. In our case, using light scattering and with particles of ~ 1-μm diameter, we measure scattering at angles (in the suspension medium) $\sim 25°$. Thus we are not observing the $k_\nabla = 0$ plane in reciprocal space. This has important implications for the effects on the observed scattering of stacking faults in the crystal structure, as is pointed out in Ref. [15], and as we comment upon further below.

III. RESULTS

A. Optical microscopy

We show first some qualitative observations of the development of shear-induced structure in the PMMA glasses, as studied directly by optical microscopy. The shear cell used in the time-resolved light scattering experiment is specifically designed also to be used in the microscope. We have described some previous microscopy experiments (using a slightly different shear cell) on the crystallization of samples at lower volume fractions in Ref. [5]. Briefly we use phase contrast microscopy [16] with a 100× oil immersion objective, ''eyepiece'' lenses of various magnifications, and video-image-capture hardware to obtain pictures of the shear induced structure in the velocity-vorticity plane. By scanning the objective vertically it is also possible to study the registration of layers in the gradient direction. Note, however, that the high magnification objective lens has a limited working distance such that it is not possible to see deeper than about 50 μm into the sample below the top plate of the shear cell. This means that at the amplitudes and frequencies used in these experiments the velocity of the imaged plane is so high that it is not possible to obtain blur-free images except at the ends of the cycle (at low frequency), or otherwise only when the shear is momentarily stopped (at higher frequency). Nevertheless direct microscopy proves to be useful in interpreting scattering observations and in studying local disorder in the shear-induced crystal structures. Figure 4 shows a sequence of images taken at intervals during a shear experiment, demonstrating the development of order in the plane imaged. In this case $\Phi = 0.585$, the strain $\gamma = 0.49$ and the frequency is $f = 5$ Hz. The plane imaged is 30 μm below the top plate, while the gap between the plates is 600 μm. The plane imaged is nearly-completely ordered within 8 min or so of shear. Scanning the objective up and down shows that similar order is visible at all heights as far into the sample as is accessible (i.e., down to 50 μm below the top). However, the shear-induced order is locally far from perfect. In Fig. 5, using a higher magnification ''eyepiece'' lens in front of the camera, we show two examples of local disorder, i.e., vacancies and dislocations.

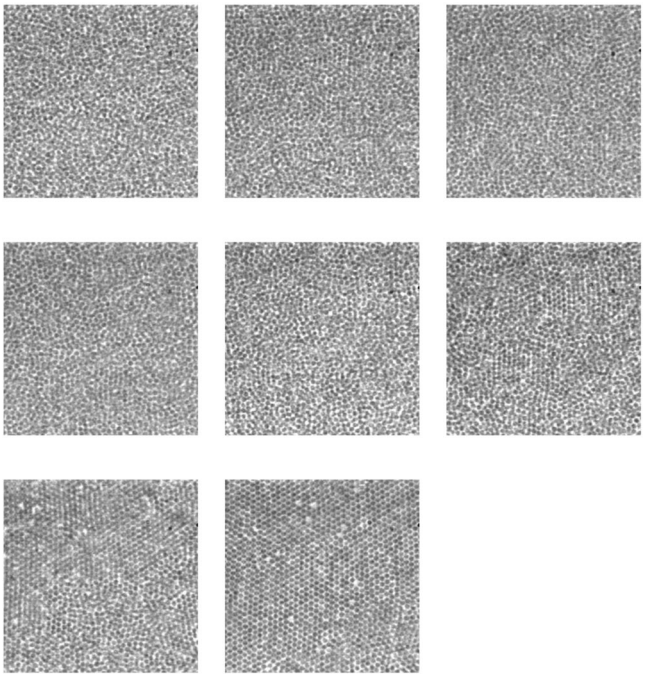

FIG. 4. Optical microscope (100× objective plus 1.6× ''eyepiece'' lens) pictures of the evolution of order in a glass sample at $\Phi = 0.585$, for an experiment at strain $\gamma = 49\%$, frequency $f = 5$ Hz. The plane imaged is 30 μm below the top plate, while the gap between the plates is $h = 600$ μm. The particles have a diameter ~ 970 nm, so that each picture is approximately 43 μm square. The velocity axis is horizontal in the pictures. The first picture (top left) is immediately before starting the shear. Subsequent times are (top row) 1 min 50 s, 3 min 5 s; (middle row) 4 min 5 s, 5 min 15 s, and 6 min 30 s; (bottom row) 7 min 30 s and 8 min 30 s. Note that these pictures were obtained by momentarily stopping the shear (typically for less than 5 s) and ''grabbing'' a digitized video image.

Scattering results indicate that the shear-induced crystals always include a substantial number of stacking faults: given the particle size and incident wavelength used here, we would not expect to see strong scattering at all for a *perfect* face-centered-cubic (fcc) structure with (111) planes aligned

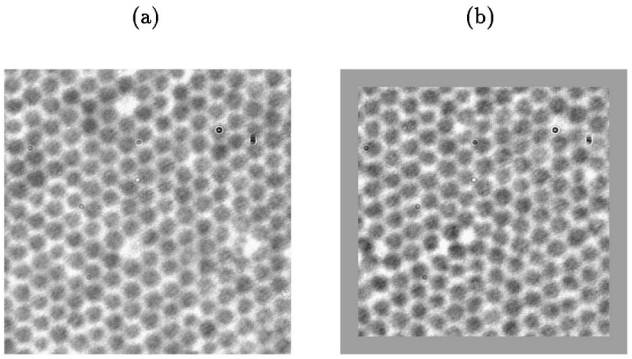

FIG. 5. Optical microscope (100× objective plus 4× ''eyepiece'' lens) pictures showing some examples of local disorder in shear-ordered suspensions. The particles have a diameter ~970 nm, so that the pictures are approximately 13 μm square. In this experiment a sample at $\Phi=0.585$ was subjected to shear at strain $\gamma=49\%$, frequency $f=5$ Hz, for 11 min; the pictures were taken after cessation of shear. The velocity axis is horizontal. (a) Hexagonally ordered plane at 30 μm below the top of the sample, containing two vacancies. (b) Hexagonally ordered plane containing a dislocation.

in the shear plane [15]. It is possible that shearing for much longer times may ''anneal'' the structure, generating perfect fcc crystals, but, as discussed, sedimentation means we are not able to carry out very long-time experiments. Further shearing might also anneal local in-plane disorder such as vacancies, dislocations, or grain boundaries. Vacancies seem to be very common in the sheared glasses, though we have yet to make any detailed or quantitative study of the local disorder. Quantitative studies are hampered by the limited area which can be observed in the microscope, which is where scattering methods are at an advantage. However, conversely, the study of local effects by scattering is problematic; a combination of direct imaging and scattering is probably the best way to proceed. Thus far, due to the high imaged plane velocity under shear mentioned above, direct study of the microscopic ordering process has not been possible. However, this could be addressed in future work by using a cell in which both the top and bottom plates are oscillated, so that a near-stationary plane may be brought within imaging range of the microscope objective.

B. DWS-echo experiments

DWS-echo experiments were carried out on samples at volume fractions $\Phi=0.57$ and 0.585. The uncertainty in the volume fraction is typically ± 0.003. (Note that at $\Phi=0.57$ experiments are performed on *metastable fluid* samples; that is, the samples are fully mixed before loading into the shear cell, and the experiment is started immediately, no more than two minutes after loading. At $\Phi=0.57$ it is at least 2 h after loading before equilibrium crystals are observed in the absence of shear.) In each experiment the data are obtained by averaging over a run lasting 5 min. At peak to peak strain $\gamma=0.05$ the oscillation frequency is 100 Hz; at higher strain for the higher volume fraction the frequency is 60 Hz.

Plots of $g_2(\tau)-1$ for the various volume fractions at $\gamma=0.05$ are given in Fig. 6. At $\gamma=0.05$ we observe a small decay of the echoes. The degree of decay is consistent with approximate measurements of the decay over the same time

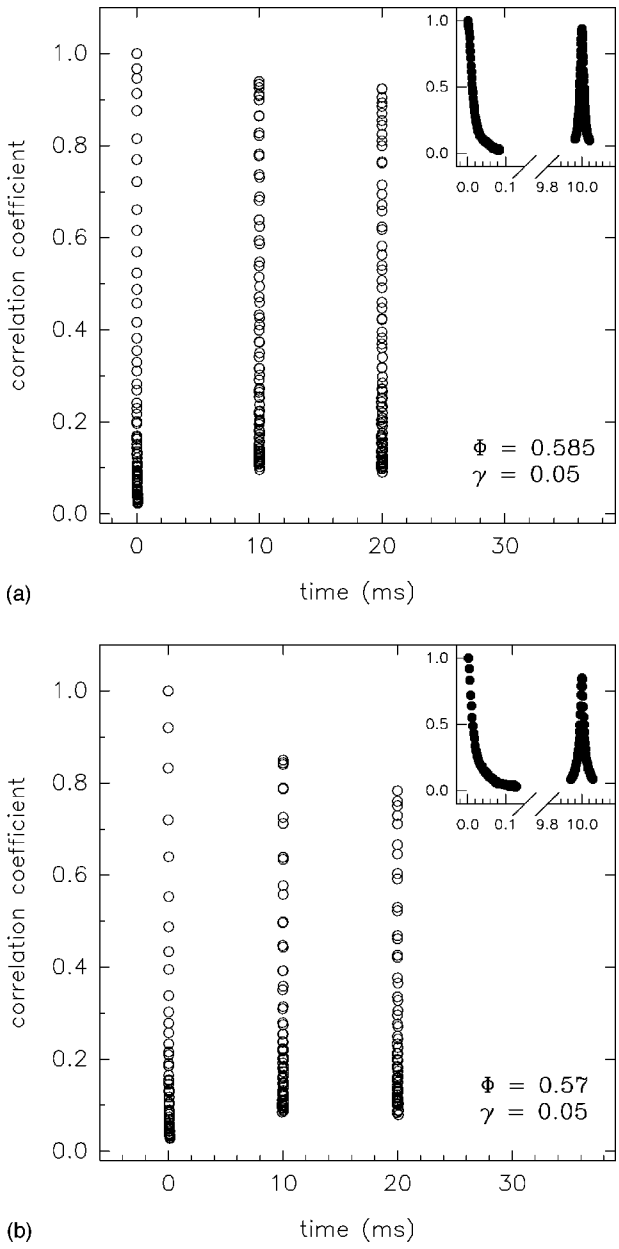

FIG. 6. Correlation functions g_2-1 from DWS-echo experiments, on samples at volume fractions (a) $\Phi=0.585$ and (b) $\Phi=0.57$, at peak to peak strain $\gamma=0.05$. g_2-1 is normalized such that its value at the smallest decay time is 1. Two echoes (i.e., correlations over one and two cycles of shear) are shown. The insets show the same data on a finer scale with broken axes, demonstrating the peak shapes.

of the correlation function *without* shear; thus we attribute this to the small amount of Brownian motion (i.e., thermal diffusion) in the samples rather than to structural changes induced by shear. Figure 7 shows the effect of increasing strain. In the case of $\Phi=0.585$ [Fig. 7(a)] *the observed decay remains approximately the same up to* $\gamma=0.2$, supporting the above interpretation that the small decay observed at low strains is *not* induced by the shear. By $\gamma=0.3$ we begin to observe an additional, though still small, decay of the echo. By $\gamma=0.475$ there is substantial decay: the first echo decays to about 0.7. We conclude that at this volume frac-

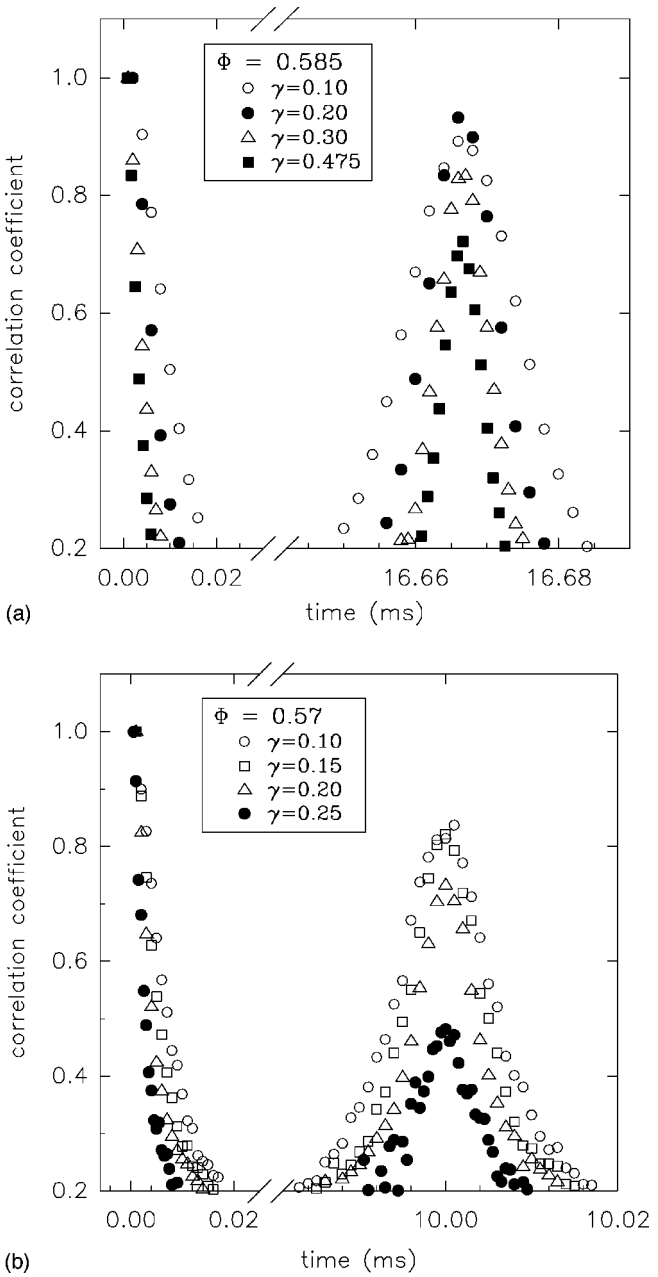

FIG. 7. Correlation functions g_2-1 from DWS-echo experiments on samples at volume fractions (a) $\Phi=0.585$ ($f=60$ Hz) and (b) $\Phi=0.57$ ($f=100$ Hz). Here we compare the first echo for a range of peak to peak strains γ. Note that for $\gamma=0.475$ at $\Phi=0.585$, the frequency was actually $f=25$ Hz; for the purposes of qualitative comparison we have rescaled the $\gamma=0.475$ time values by $\frac{25}{60}$. The error bars on the echo peak heights can be judged from the variation of echo height in (a) for $\gamma=0.1$ and $\gamma=0.2$, as about ± 0.03.

tion, just above the glass transition $\Phi_g=0.58$, on length scales down to the order of a fifth of the particle radius (the length scale sensitivity determined by the turbidity of the samples), *the hard-sphere glass strains approximately reversibly up to peak to peak strains of at least 20%*.

That the glass is able to strain reversibly up to 20–30 % strain is somewhat surprising. The comparison with the behavior at $\Phi=0.57$, just below the glass transition, is striking [Fig. 7(b)]. At $\Phi=0.57$, already by $\gamma=0.2$ there is observable decay of the echo, and by $\gamma=0.25$ the echo has decayed to 0.5. Thus the behavior of the samples is clearly strongly dependent on volume fraction near the glass transition.

In very viscous systems such as the PMMA glasses, at strains as high as 30%, fracture of the sample might be supposed possible. In fact, as will be discussed in Sec. III C, in the time-resolved light scattering experiments we do observe possible evidence of fracture (that is high strains localized at ''slip'' planes) at higher volume fraction, $\Phi=0.599$. However, at $\Phi=0.587$ and 0.569, corresponding to the volume fractions studied in the DWS-echo experiments, the time-resolved light scattering experiments show no evidence of such fracture. In fact approximate measurements of the velocity profile in the sheared glass samples by optical microscopy show no evidence of any strong nonlinearity, at least in the visible part of the sample near the top (see above), thus it seems that the strains quoted for the DWS-echo experiments (which assume a linear velocity gradient, i.e., $\gamma=A/h$) are meaningful.

The comparison of these data for PMMA hard-sphere particles with the observations of Hebraud *et al.* [1] for ''soft emulsion'' glasses is interesting. First, a significant decay of the echo and so significant shear-induced structural changes were observed in the emulsions at much lower strains (even though the volume fractions were higher) than in the PMMA glasses. Furthermore, in the emulsions the fact that, after a decay over the first cycle, subsequent echoes (i.e., on longer time scales) did not decay any further, was interpreted as indicating a ''localized yielding'' of the sample: those parts which yielded irreversibly during the first cycle continued to yield, whereas parts of the sample which strained reversibly on a time scale of one cycle continued to strain reversibly over many cycles. Unfortunately study and interpretation of echoes over much longer time scales is more difficult in our experiments due to the greater degree of thermal diffusion, which leads on long-time scales to a substantial decay of the echo independent of the shear. (As mentioned, even at short-time scales, e.g., one or two cycles, a small decay is visible, as in Fig. 6.) In the emulsion systems volume fractions were typically $\sim$70–80 % and thermal diffusion nearly completely absent. Of course the effectively nondeformable PMMA particles cannot be easily concentrated beyond about $\Phi\sim 64\%$, the random close packing fraction of hard spheres. Careful measurement of and compensation for the decay of correlation due to thermal diffusion might enable study of shear-induced yielding at longer time scales, but we have not attempted this so far. Precise measurement of the zero-shear correlation function of the nonergodic glassy samples requires repeat experiments to obtain a correct ensemble average.

C. Time-resolved static light scattering

We now examine the shear-induced ordering behavior of the glasses and compare with the conclusions drawn from the DWS-echo experiments. Time-resolved light scattering experiments were carried out on samples at volume fractions $\Phi=0.569$, 0.587, and 0.599. All experiments were carried out at a frequency of 5 Hz. Plots of the peak diode voltage (proportional to the scattered light intensity) vs time are given in Fig. 8, for each volume fraction at various strain

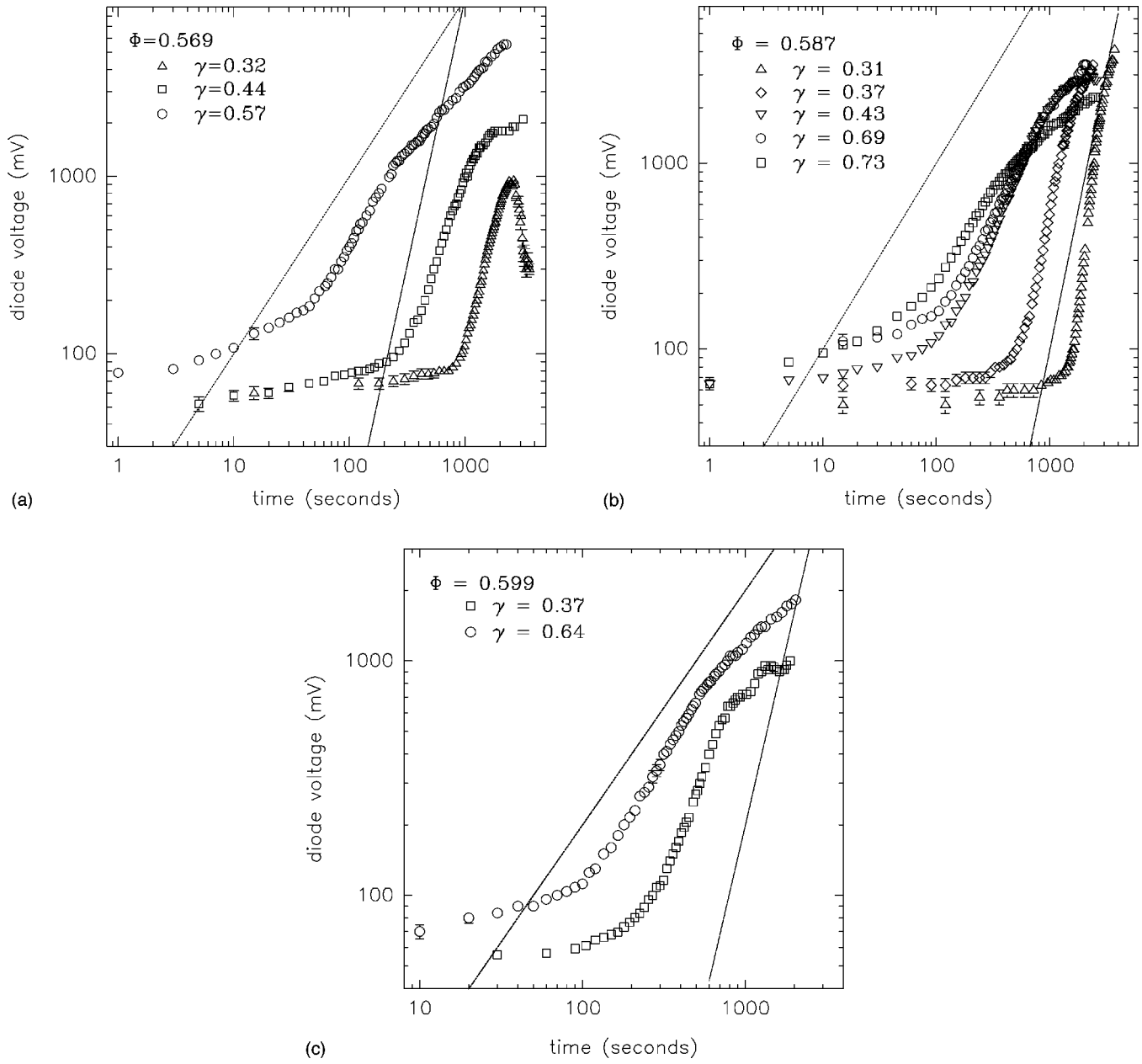

FIG. 8. Photodiode peak voltage (proportional to scattered intensity) as a function of time in time-resolved static light-scattering experiments for samples under shear at various volume fractions and peak to peak strains. Time is measured from the start of shear. (a) $\Phi = 0.569$, (b) $\Phi = 0.587$, and (c) $\Phi = 0.599$. See text for discussion of the linear (t) and t^3 lines also shown.

amplitudes. In general we have not continued experiments for longer than 40–60 minutes due to the possibility of sedimentation of the particles affecting the kinetics of the growth.

Typically we observe the following features in the increase of the scattered intensity. At early time there is an ''induction'' period of very slow (or nearly no) increase in intensity. Presumably this is related to the slow induction or nucleation of crystal order. Subsequently a fast increase of intensity is observed. This increase occurs at about the same time as the appearance in the scattering pattern of the strong ''lobes'' indicating the development of aligned, ordered structure (Fig. 3). For the higher strains, as they become brighter the lobes also quickly become less extended around the scattering ring, presumably as more order is generated which is more nearly aligned with the velocity axis. However, at the lowest strains we observe a somewhat different development of the scattering pattern. Typically to begin with faint lobes are observed, only just visible against the fluid scattering, and often *on the velocity axis alone*. The extent of these lobes around the velocity axis is usually much smaller than the initial extent of the lobes observed at higher strain. At later times the ''off-axis'' lobes also become visible, but generally these remain less intense than the lobes on the velocity axis. In addition, for the glasses there remains always significant scattered intensity around the ''fluid'' ring between the bright lobes, indicating that ordering in the glasses is not complete and parts of the sample remain fluid rather than crystal, at least up to the time scales of our experiments.

Differences with strain are apparent in the behavior of the measured intensity. The ''induction'' time t_i increases

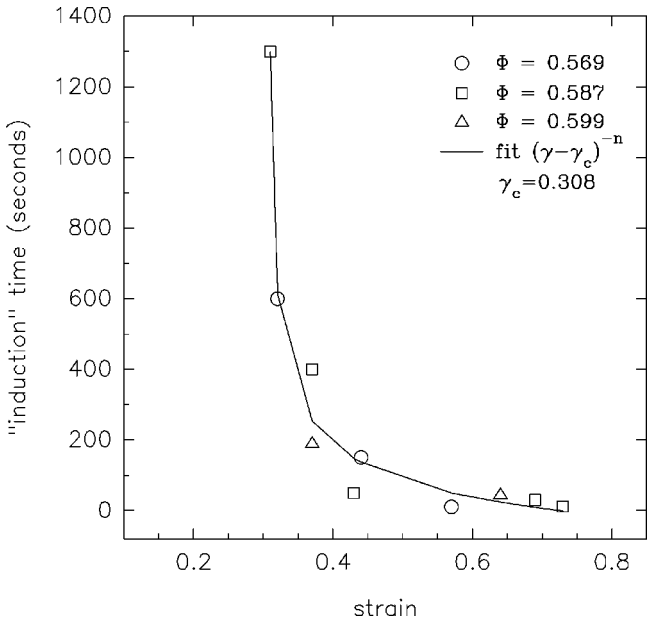

FIG. 9. ''Induction'' time for onset of fast growth of scattered intensity, as a function of strain. Data from three volume fractions are plotted on the same graph. The line illustrates a fit (to *all* data) of the function $t_i = t_0 + (\gamma - \gamma_c)^{-n}$. The best-fit parameters obtained are $\gamma_c = 0.3$ and $n = -0.27$. See text for discussion.

sharply with decreasing strain. In Fig. 9 we plot the estimated t_i against strain for each volume fraction. t_i was estimated by two methods: backward extrapolation of the steep slope (i.e., late time) portion of the curves to the time axis; and estimation from the crossing point of two straight lines going approximately through the early and late time portions of the curve. Both methods of estimation give similar results for the behavior of t_i with strain; for clarity, Fig. 9 shows results only from the first method. We observe something like a divergence of t_i as strain γ decreases toward some critical value γ_c. The results of the DWS-echo experiments lead us to expect a γ_c dependent on volume fraction (compare the strains at which significant decay of the DWS echo is first observed for $\Phi = 0.585$ and 0.57, Fig. 7). Given the small number of data points estimation of γ_c separately for each volume fraction is difficult. Attempts to fit a function of the form $t_i = t_0 + (\gamma - \gamma_c)^{-n}$ to the data for $\Phi = 0.587$ alone demonstrated that the fitted γ_c was very sensitive to the starting estimate used for the least-squares procedure. Instead, as no more than an illustration, we have shown in the figure a line fitted to *all* data (i.e., from all three volume fractions). In any case the data from the samples at $\Phi = 0.587$ are consistent with the observations from the DWS-echo experiments at $\Phi = 0.585$, that there is a peak to peak strain $\gamma_c \sim 25$–$30\,\%$ below which crystal order cannot be induced, because the sample strains reversibly.

After ''induction,'' there are further differences in the behavior of the scattered intensity at different strain. At lower strain, having waited a longer ''induction'' time, growth of order now appears to be significantly *faster*. In Fig. 8 we have drawn lines corresponding to linear (dotted lines) and t^3 (full lines) growth for comparison with the data. As can be seen, as strain decreases there is a tendency for the increase of intensity to speed up from approximately linear in time to approximately t^3 or even faster. In equilibrium classical nucleation theory a t^3 increase in crystal volume (or linear increase in crystal size) is indicative of interface-limited (as opposed to diffusion-limited) growth, which is perhaps what we might expect given that the interlayer strain is driving the ordering process. On the other hand, an approximately linear increase followed by a slowing down might indicate a nucleation ''burst'' and a subsequent ripening of touching crystals. However, given the semiquantitative character of the measurements (i.e., we have not subtracted scattering from the fluid part of the sample, nor have we considered possible effects of multiple scattering, etc.) and the limited duration of the experiments, we refrain from directly estimating or interpreting growth exponents. At any rate the trend for longer induction time followed by faster growth as strain decreases is clear, and is observed at all volume fractions studied.

The apparent rate of increase of order in equilibrium (i.e., zero-shear) homogeneous crystallization of PMMA suspensions has been studied by Harland and van Megen [17]. Growth is found to be faster at lower *volume fraction*, attributed to the idea that at a lower nucleation rate isolated nuclei can grow without competition, and growth is not interfered with by continuing rapid nucleation between existing growing nuclei. A similar idea may apply to shear-induced nucleation at lower strains, where again we might expect a lower density of nuclei. However, it is also possible that at high strain more crystallites are nucleated further from precise orientation along the velocity axis; these crystallites will scatter to either side of the velocity axis, and some of the scattered light will not be picked up by the diode on the axis. Thus the apparently slower growth at higher strains may be a result of a strain-dependent distribution of orientations of crystallites. Unfortunately, a quantitative measurement of a larger portion of the scattering pattern is more difficult due to the requirement for a large-area detector with a wide range of linear response. Most conventional (i.e., low-cost) video cameras, for instance, have a linear range of at best 1.5–2 decades, and are not suitable for a quantitative measurement. It remains to study the evolution and strain dependence of the distribution of crystallite orientations in more detail in future work. Meanwhile, our interpretation of the kinetic measurements remains tentative. It is worth noting though that calculation of quantities comparable to our measurements from computer simulation of shear ordering in suspensions [18] ought to be straightforward, and should lead to more powerful tests of simulation models against experiment.

At the highest volume fraction studied, $\Phi = 0.599$, we observe in many experiments not only the ''lobe'' pattern as in Fig. 3 but another hexagonal set of six *sharp* peaks (*not* lobes), rotated by 30° relative to the lobe pattern. These peaks are generally much less bright than the lobes, and do not seem to increase in brightness very quickly. Moreover, they generally appear within less than a minute of commencing the shear, even in those cases where the lobe pattern does not become visible for a long ''induction'' time. The orientation of the six sharp peaks indicates the formation of hexagonal planes whose close-packed direction is oriented *parallel* to (rather than perpendicular to) the velocity axis. Such a pattern is normally observed in experiments at strains $\gamma \gg 100\%$ (and in steady shear experiments): at $\gamma \gg 100\%$ the

suspension is proposed to strain most easily via a ''zigzag'' sliding motion of planes aligned with a close-packed direction parallel to the velocity [2,3]. Such a mixture of ''low-strain'' lobes and ''high-strain'' or ''sliding layer'' order was also previously observed for a PMMA glass at $\Phi = 0.595$ by Ackerson [3]. Careful observations in our experiments indicate that there is no macroscopic flow or shape distortion of the sample. Therefore, the most likely explanation of the apparent formation of high-strain-like order in a low-strain experiment seems to be that the sample suffers *fracture*. Slip or fracture between two adjacent planes would represent effectively a *locally* high strain (relative movement of the two planes of more than a particle diameter would be enough to make the local strain greater than 100%), in response to which the particles in planes near the ''fault'' would tend to order in the high-strain orientation. That we observe the high-strain peaks very early in the experiment (regardless of the apparent overall γ) indicates that the fracture may be due to the failure of the glass to relax quickly enough the sharp stress applied when the shear is first started. This idea is further supported by the observation that such high-strain peaks are never observed at $\Phi = 0.57$, and only very seldom in experiments at $\Phi = 0.585$. In any case, this fracture effect deserves further study. It remains unclear to what extent fracturing is local, or is even possibly associated with the surfaces of the cell. Direct observation and measurement of velocity profiles by optical microscopy would perhaps be a useful approach. It remains difficult, however, as discussed, e.g., in Ref. [5], to measure the complete velocity profile at the amplitudes and frequencies involved here, due to the conflicting requirements of high resolution and wide field of view (such that micron-sized particles may be resolved and tracked at high velocity across a significant portion of the oscillation cycle).

Late-time behavior of the scattered intensity is somewhat erratic. An example can be seen in Fig. 8(a) for the lowest strain, $\gamma = 0.32$, where at late time the intensity falls substantially. The late-time structural behavior of the samples has been observed by microscopy to be complicated [5]: for example the grains at different orientations start to interact, causing sliding along grain boundaries and rather complex evolution of large-scale structure. Scattering experiments often do not give very repeatable results at late times. Moreover late-time behavior of the samples may also be affected by problems such as sedimentation. Given these points it is clear that further study is required before we may obtain a reasonable picture of late-time behavior.

IV. CONCLUSIONS

DWS-echo experiments show that colloidal hard-sphere glasses appear to deform reversibly under (peak to peak) oscillatory shear strains as high as 20–30 % (for $\Phi = 0.585$, just above Φ_g). Consistent with these experiments measurements of the ''induction'' time for shear-induced crystallization show a divergentlike behavior of the induction time as strain is decreased toward $\sim 30\%$. At strains of $\gamma = 30$–$70\,\%$, measurements of the growth rate of crystal order demonstrate a sensitive dependence on γ, growth being faster (after longer induction time) at lower strain. This may be an apparent effect due to the nucleation of crystallites with a distribution of orientations which is wider at higher strain. However, optical microscope studies are broadly consistent with an extended induction time during which little order is observed, followed by quite fast appearance of near-complete order in the imaged plane of the sample (Fig. 4). At the highest volume fractions samples display a tendency to fracture, generating both low-strain order ($\gamma < 100\%$) and local high-strain order ($\gamma \gg 100\%$). Finally, optical microscope observations show that the shear-induced order in PMMA glasses is not locally perfect, vacancies and dislocations being common. Given that crystallites nucleate independently at different places, one would expect to find local disorder where the growing nuclei meet and begin to ''compete.'' A higher nucleus density may also be partly responsible for the slower observed rate of growth of order at higher strain.

A truly microscopic picture of the structural effects of shear in concentrated colloidal suspensions is still lacking. Perhaps the most obvious route to a detailed structural picture on the scale of single particles is by computer modelling. More detailed comparison of simulation results, for instance with kinetic data from experiments such as those described here, would enable better confidence in simulation models. In experiments meanwhile, optical microscopy, in particular of suspensions under shear, would seem to have great potential for future development and exploitation.

ACKNOWLEDGMENTS

We thank M. E. Cates, P. Sollich, and J. P. Munch for useful discussions, and A. B. Schofield and V. Trappe for the synthesis of the PMMA particles. M.D.H.'s work was funded by the U.K. Engineering and Physical Sciences Research Council (EPSRC). The optical microscopy was carried out using equipment purchased with grants from the Royal Society and from the EPSRC.

[1] P. Hebraud, F. Lequeux, J. P. Munch, and D. J. Pine, Phys. Rev. Lett. **78**, 4657 (1997).

[2] W. Loose and B. J. Ackerson, J. Chem. Phys. **101**, 7211 (1994).

[3] B. J. Ackerson, J. Rheol. **34**, 553 (1990).

[4] B. J. Ackerson and P. N. Pusey, Phys. Rev. Lett. **61**, 1033 (1988).

[5] M. D. Haw, W. C. K. Poon, and P. N. Pusey, Phys. Rev. E **57**, 6859 (1998).

[6] The shapes and size distribution of crystalline grains grown under shear in a dilute suspension of charged particles have been studied by T. Palberg, W. Monch, J. Schwarz, and P. Leiderer, J. Chem. Phys. **102**, 5082 (1995).

[7] P. N. Pusey, in *Liquids, Freezing and the Glass Transition*, edited by J. P. Hansen, D. Levesque, and J. Zinn-Justin (Elsevier, Amsterdam, 1991).

[8] W. van Megen and P. N. Pusey, Phys. Rev. A **43**, 5429 (1991); W. van Megen and S. M. Underwood, Phys. Rev. E **49**, 4206 (1994).

[9] See, e.g., S. E. Paulin and B. J. Ackerson, Phys. Rev. Lett. **64**,

2663 (1990); P. N. Segre, O. P. Behrend, and P. N. Pusey, Phys. Rev. E **52**, 5070 (1995).

[10] J. Zhu, M. Li, R. Rogers, W. Meyer, R. H. Ottewill, STS-73 Space Shuttle Crew, W. B. Russel and P. M. Chaikin, Nature (London) **387**, 883 (1997).

[11] F. Renth and M. D. Haw (unpublished). An important problem is that while detailed long term investigation has shown the PMMA particles to be completely stable in decalin, many other solvents appear to cause swelling of the PMMA particles (or of the steric stabilizing layer), thus making a determination of the particle volume fraction problematic.

[12] G. Maret, Curr. Opin. Colloid Interface Sci. **2**, 251 (1997); D. A. Weitz and D. J. Pine, in *Dynamic Light Scattering*, edited by W. Brown (Oxford University Press, New York, 1993).

[13] Y. D. Yan, J. K. G. Dhont, C. Smits, and H. N. W. Lekkerkerker, Physica A **202**, 68 (1994).

[14] See e.g. C. G. de Kruif, J. C. van der Werff, S. J. Johnson, and R. P. May, Phys. Fluids A **2**, 1545 (1990); B. J. Ackerson, J. B. Hayter, N. A. Clark, and L. Cotter, J. Chem. Phys. **84**, 2344 (1986); P. Lindner, Physica B **180**, 499 (1992).

[15] J. Liu, D. A. Weitz, and B. J. Ackerson, Phys. Rev. E **48**, 1106 (1993).

[16] M. Pluta, *Advanced Light Microscopy* (Elsevier, Amsterdam, 1989), Vol. 2.

[17] J. L. Harland and W. van Megen, Phys. Rev. E **55**, 3054 (1997).

[18] See, e.g., W. Xue and G. S. Grest, Phys. Rev. Lett. **64**, 419 (1990); S. Butler and P. Harrowell, Phys. Rev. E **52**, 6424 (1995); H. Komatsugawa and S. Nose, *ibid.* **53**, 2588 (1996).